Air trench waveguide bend for high density optical integration

Shoji Akiyama*[a], Kazumi Wada[a], Jurgen Michel[a], Lionel C. Kimerling[a], Milos A. Popovic[b], Hermann A. Haus [b]
[a] Massachusetts Institute of Technology, Department of Materials Science and Engineering, 77 Massachusetts Avenue, Cambridge, MA 02139;
[b] Massachusetts Institute of Technology, Department of Electrical Engineering and Computer Science, 77 Massachusetts Avenue, Cambridge, MA 02139

ABSTRACT

Air trench structure for reduced-size bends in low (Δn=0.01-0.1) and medium (Δn=0.1-0.3) index contrast waveguides is proposed. Local high index contrast at bends is achieved by introducing air trenches. An air trench bend consists of cladding tapers to avoid junction loss, providing adiabatic mode shaping between low and high index contrast regions. Drastic reduction in effective bend radius is achieved. We present FDTD simulations of bends in representative silica index contrasts, fabrication scheme and waveguide loss measurement results using Fabry-Perot loss measurement technique. We employed CMOS compatible processes to realize air trench bends and T-splitters to achieve low production cost and high yield. A simple, compact waveguide and T-splitter are fabricated and evaluated. The loss measurement results show that losses are consistent with theoretical simulations. By using air trench waveguides, other applications such as BioMEMS (e.g. Evanescent-field sensor) or EDWA can be realized.

Keywords: air trench bend, cladding taper, silica waveguide, bend loss, low index contrast, enhanced lateral mode confinement

1. INTRODUCTION

Low index contrast (LIC) silica bench technology which is often referred to as PLC (planar lightwave circuit) or SiOB (silica optical bench) has been widely used in practice in the fabrication of passive integrated optical components such as arrayed waveguides gratings (AWGs) by virtue of its use of well-tested CMOS processes and technology [1]. It has been reported that LIC platform provides low fiber-to-chip coupling and propagation losses due to its low index contrast between core and cladding [1]. But a major drawback of LIC platform is the relatively large footprint, where a critical factor is the minimum waveguide bend radius. This radius is as large as in the millimeter or centimeter order (Δ = 0.25-1.5%) [1] depending on its index contrast. Low density of integration keeps production cost high, and invites yield problems and also temperature instability for AWG application due to its large size. On the other hand, high index contrast such as Si/SiO_2 or SiN/SiO_2 material system where the index difference is as much as 2 or 0.5-0.7, respectively, while offering dense integration, poses challenges of fiber-to-chip insertion loss due to mode shape mismatch and misalignment between fiber and waveguide, scattering loss and vulnerability to other fabrication defects and tolerances, as well as fabrication processing challenges such as lithography capability. Air trench waveguides offer a drastic reduction in the bending radius, while offering simple fabrication, and the size problem of PLC platform will be overcome. Truly large-scale optical integration will be achieved on low, middle index contrast platform using our proposed structures.

*akiyama@mit.edu; phone 1(617)253-6907; fax 1(617)253-6782; http://photonics.mit.edu/

Integrated Optics: Devices, Materials, and Technologies VIII,
edited by Yakov Sidorin, Ari Tervonen, Proceedings of SPIE Vol. 5355
(SPIE, Bellingham, WA, 2004) · 0277-786X/04/$15 · doi: 10.1117/12.529630

2. BACKGROUND

By using effective index (EIM) method or other standard semi analytical tools [2-6], the 98% transmission radius, R98, can be calculated. Fig.1 depicts R98 for various optical waveguides. According to Fig.1, it can be seen that small bending radius with small radiation loss is achieved by increasing index difference between core and cladding. It seems that high index contrast (HIC) platform is the natural choice to achieve dense integration of optical components, but high index contrast waveguides usually have high propagation loss which is caused by sidewall roughness of the waveguide [7-8] which is formed during dry etching process. And poor coupling between fiber and waveguide due to mode shape mismatch and its sensitive alignment are also fundamental problems for HIC platform. It is reported that propagation loss is proportional to the 3rd power of the sidewall roughness [7-8]. On the other hand, LIC waveguides provide small propagation loss and excellent fiber-to-chip coupling but have to have relatively large bending radius to achieve low bend loss. This size problem is critical for the dense integration of optical components. As another candidate for dense integration, photonic crystal bandgap (PBG) waveguides are attracting considerable attention for the purpose of the dense integration of optical waveguides [9-11]. But due to poor vertical mode confinement and fabrication problems, they usually show high propagation loss. Recently the use of medium index contrast waveguide has been proposed where index difference ranges from Δn=0.05-0.3 to avoid the problems of high index contrast and low index contrast waveguides [12-17]. But the bend radius is still a problem for dense integration. For example, when index difference is Δn=0.1(Δ=7%), 100-200μm radius is required to achieve 98% transmission (0.09dB loss) for right turn. Therefore, it can be concluded that there is no fundamental solution using conventional waveguide designing techniques. We propose a new scheme using air trenches to provide locally enhanced lateral confinement at bends and at T-splitter. We use adiabatic tapering to avoid abrupt junction-induced mode mismatch and Fresnel reflection in order to miniaturize optical waveguide bends while preserving low-loss performance [18]. The basic scheme of air trench bend is depicted in Fig.2. We propose simple structures to achieve compact waveguide system for future microphotonics and other applications.

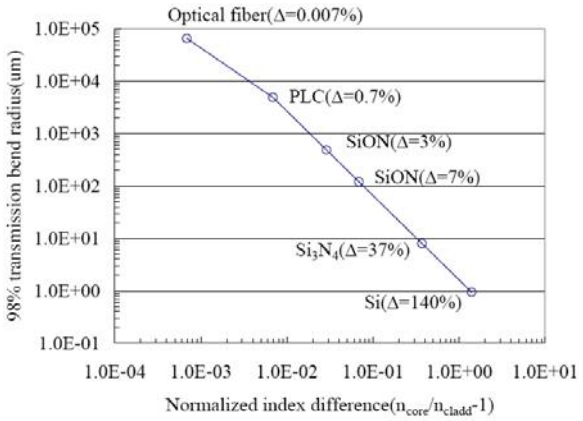

Fig. 1. 98% transmission bend radius(R98) –Calculation is based on EIM method. Claddings are assumed to be silicon dioxide(SiO_2)

3. Air Trench Bend Theory and Simulations

Theoretical details of air trench bend design are discussed in [18]. In straight propagation, the structure is a simple low index contrast channel waveguide (cross section A in Fig. 2a). At bends, air trenches are placed to enhance lateral

mode confinement by introducing local high index contrast (cross section B in Fig. 2a). To avoid junction loss between the straight and bending sections, an adiabatic taper is placed at the input and output junction. These adiabatic tapers provide fast mode transition between straight and bending waveguides. This type of air trench bend can result in a drastic reduction in bending radius depending on the index contrast between core and cladding. Fig. 3 summarizes bend size for conventional waveguide bends and air trench bends for the case of 0.088dB loss, which is corresponding to 98% transmission [18]. Three examples (A,B,C) in Fig.3 depict the case where $\Delta(n_{core}/n_{cladding}-1)$ = 0.25%, 0.68% and 6.8% , respectively. The result is a theoretical reduction in bending radius by a factor of 10-1000 and in total bend structure edge length by a factor of 4-60. Simulations were done using the 2D FDTD.

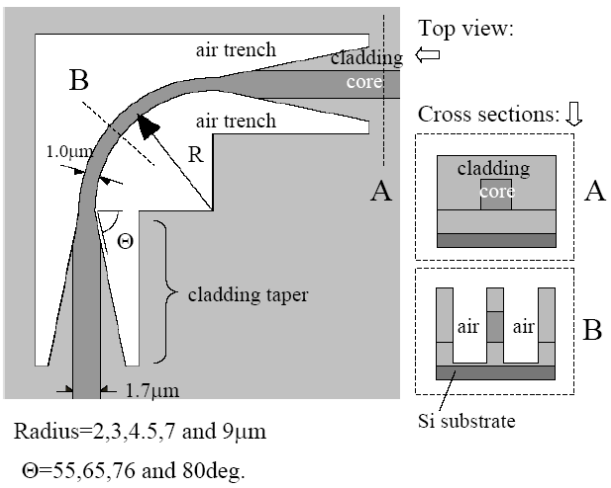

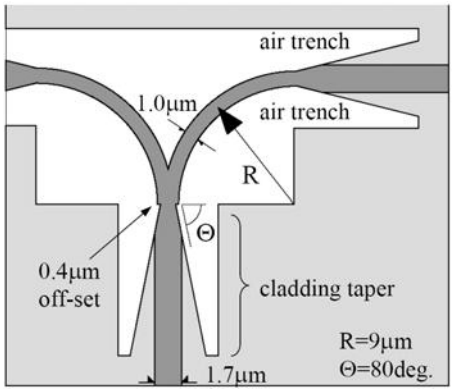

Fig.2a. (left): Air trench bend schematic – (A) Cross sectional view of low index (straight) waveguide, (B) Air trench region (bend)

Fig.2b. (right): Air trench T-splitter schematic: Radius and Taper angle are fixed at 9mm and 80deg, respectively

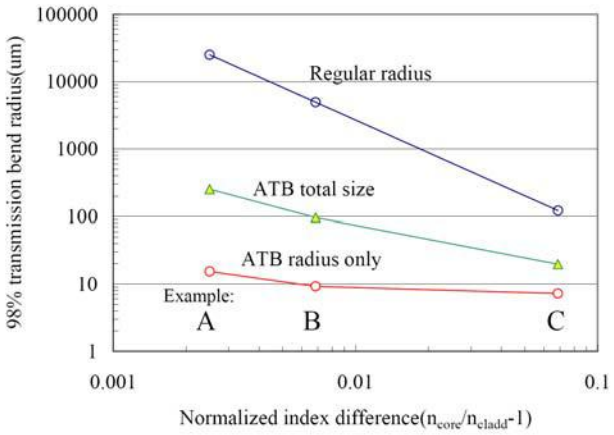

Fig.3. 98% transmission bend radius(R98) for conventional bend and air trench bend

4. Design parameters

For the fabrication of ATB and T-splitter, the index difference is targeted at Δn=0.1(Δ=6.85%: Example C in Fig.3). Silicon oxynitride (SiON) is chosen as core material since its refractive index can be easily adjusted during deposition

just by changing gas composition [17]. Radii and taper angles are varied from 2 to 9μm and 55 to 80deg. respectively as in Fig.2a since they are the most important factors for miniaturization of the bend. The widths of channel waveguide and air trench waveguide are 1.7μm and 1μm respectively to keep single mode in low index contrast (straight) region and high index contrast (bend) region. Trench depth is chosen to be 4μm to minimize substrate loss. According to our previous study [18], trench depth should be more than twice as deep as core thickness to achieve 0.01dB substrate loss. This low loss is achieved by confining all the evanescent tale of guided light inside deep air trenches.

5. Fabrication

The starting substrate was CZ grown p-type (0.1-100Ωcm) silicon wafer and the under cladding was grown by high pressure thermal oxidation process (HIPOX) at 1050ºC. After growing the under cladding, a silicon oxynitride (SiON) core layer was deposited by Plasma Enhanced Chemical Vapor Deposition (PECVD) process. The target index was 1.5456 at 1.55μm so that index difference between core and cladding is 0.1. SiON deposition was done using a Novellus Concept1. The thickness and refractive index (at 633nm) of SiON film were 2.0498μm and 1.5294, respectively as deposited. This evaluation was done by Metricon model 2010 prism coupler. The wavelengths used here were 633nm and 1550nm, in TE mode. After core layer deposition, high temperature anneal (N_2 ambient, 1050ºC 1-6 hours) was applied to densify the SiON film and to remove hydrogen atoms since it has been reported that N-H bonds work as an absorption center in the 1.55μm communication range [12]. It has been also reported that this N-H bond is introduced during deposition from reaction gas NH_3. During the annealing process, the SiON layer refractive index and thickness changed as in Figs. 4a and 4b, respectively. Both the thickness and refractive index converged to steady values after 4 hours. We assumed that all the hydrogen atoms were diffused out at this point and used SiON which had been annealed for 4 hours for the following steps. Lithography was done by i-line (365nm) stepper. After photoresist coating and exposure processes, photoresist was irradiated by UV light using Fusion M150PC Photostabilizer to avoid photoresist deformation during successive post bake. Post bake was done at 130ºC for 3min and at 200ºC for 3min on hot plate. Then waveguide was fabricated by dry etching process using the mixture of C_2F_6 and CH_3F gases. Top cladding SiO_2 was deposited also by PECVD. Chemo-mechanical polishing (CMP) was applied to obtain smooth surface for the second lithography process. Then second lithography and dry etching are done to fabricate air trench with the same procedure as the waveguide fabrication

Fig. 5 is a set of optical microscope (Zeiss axioplan) top view images of an air trench bend and T-splitter where radius is 9μm and taper angle is 80º. It can be seen that two layers (waveguide and air trench layers) are well aligned with each other. All of the dimensions were checked by SEM observation.

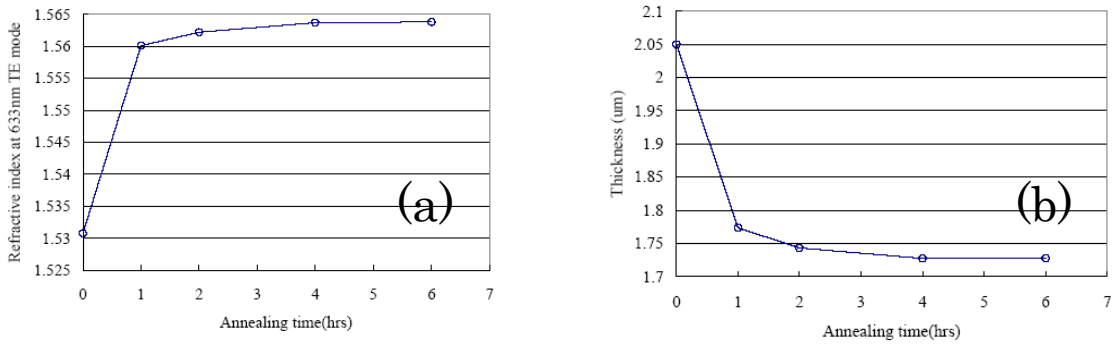

Fig.4. Properties' change during densification anneal, (a: left) Refractive index change, (b: right) Thickness change

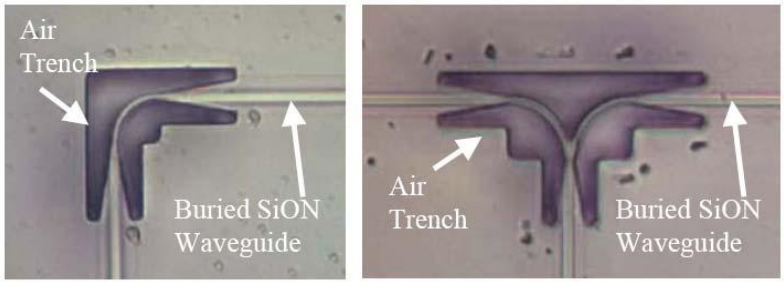

Fig.5. Optical microscope images for AT bend (left) and AT T-splitter (right)

6. Measurement results

Waveguide loss measurements were done by Fabry-Perot resonance method to obtain trustable results. Compared with the conventional cut-back method, this technique provides more precise measurement since optical contrast (Imax/Imin) does not depend on the coupling condition between optical fiber and waveguide which is very sensitive to alignment conditions [7], [19]. The loss is simply calculated from the ratio of maximum to minimum intensity according

$$\alpha = -\frac{1}{L}\left(\frac{1}{R}\ln\frac{\sqrt{I_{\max}/I_{\min}}-1}{\sqrt{I_{\max}/I_{\min}}+1}\right) \qquad (1)$$

where α is the propagation loss coefficient, L is the length of the waveguide, and R is facet modal reflectivity. Imax and Imin are the peak and bottom intensities of the Fabry-Perot spectrum, respectively. The reflectivity R was calculated by a three-dimensional finite-difference time-domain (FDTD) simulation. The input and output facets were polished using Buehler ECOMET3 system to suppress scattering at facets during measurement.

For both TE and TM modes, this waveguide showed propagation loss as low as 0.27±0.1dB/cm. Loss was obtained by averaging the results from 10 peaks and valleys in the Fabry-Perot spectrum near 1550nm.

A. Air Trench Bend Results

Figs. 6a and 6b show bending losses for a 90º air trench bend for TM ('quasi-TE' in [18], out-of-plane) and TE ('quasi-TM' in [18], in-plane) modes, respectively. In Figs.6a and 6b, cladding taper angle is fixed at 80-degrees and inner radii of the bend section are varied from 2 to 9μm. Bend loss is as small as 0.1dB/turn and matches to a reasonable degree the 2D FDTD simulation results for both polarizations. The geometry of air trenches is very well suited to approximation by 2D FDTD using the effective index method [18]. However, the experimental results have as much as ~0.15dB standard deviation. The values shown in Figs. 6a and 6b are the averages of 10 Fabry-Perot resonance points near 1550nm.

Another important factor for the miniaturization of bend while maintaining low loss is the cladding taper angle. Larger the taper angles result in lower reflection and radiation losses, but increase device size. Optimizing an adequate taper angle is key to achieving compact, low-loss bends. Figs. 7a and 7b show bending loss per 90-degree air trench bend for TM (quasi-TE) and TE (quasi-TM) modes, respectively, for several taper angles with the radius fixed at 9μm.

Experimental results match simulation with some deviation. From these results it is confirmed that taper design has a significant impact on the loss of the bend as predicted from theoretical simulation, and that cladding tapers permitting low-loss bends can be fabricated.

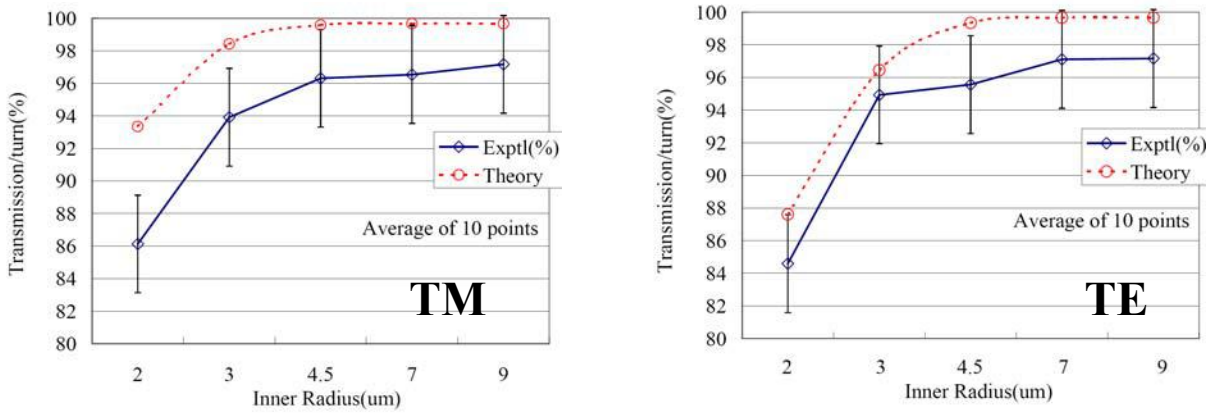

Fig.6. Bend Losses for TM (left) and TE (right) modes. Radii are varied from 2 to 9μm. Taper angle is fixed at 80deg.

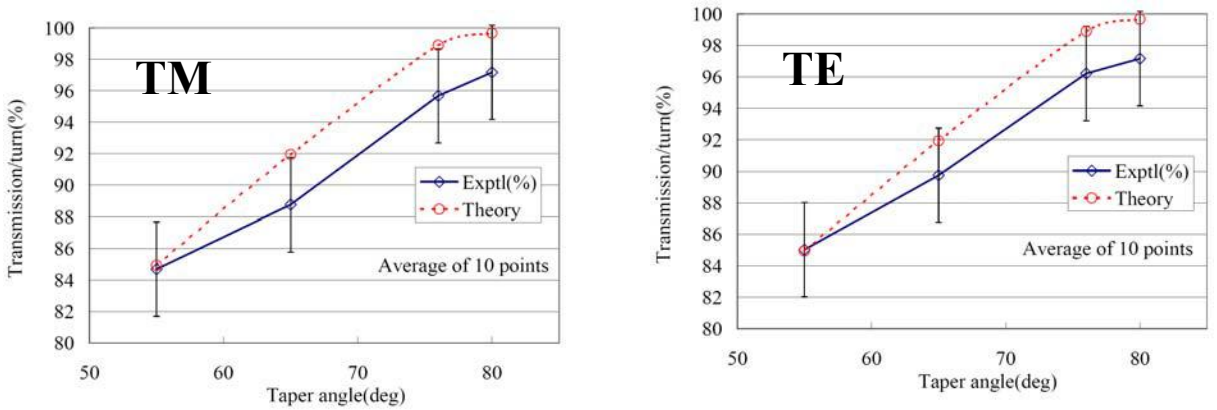

Fig.7. Bend losses for TM (left) and TE (right) modes. Taper angle is varied from 55 to 80deg. Radius is fixed at 9μm.

B. Air Trench T-splitter Results

In the T-splitter illustrated in Fig. 2b and shown in Fig.5, the radius and taper angle are fixed at 9μm and 80º, respectively. A straight throughput loss measurement was employed to find approximately less than 0.6dB loss per junction. A key factor in T-splitters is even (or controllable by design) power distribution. Even power splitting is particularly important for optical clock distribution. The splitting ratio for the device shown is around 45:55.

It was found that accurate alignment between the two structures (waveguide core and air trench structures) is an important factor for even power distribution. The splitting ratio was degraded to 30:70 for 1540-1565nm range when there is ~ 0.3μm lateral misalignment between the waveguide and air trench. By paying attention to precise alignment, compact, low-loss and evenly-power-splitting T-splitters can be realized using air trench bends. The designing

parameters were the same as the air trench bend as in Fig.2a.

7. Discussion and Summary

We presented the realization of novel waveguide structures by which sharp bend radii and dense integration can be achieved in low-index contrast waveguides while keeping propagation loss and radiation (bending) loss within acceptable bounds. By introducing local high index contrast (the air trench) at the bend gradually, away from the core first, in a configuration which allows for adiabatic mode transition from low to high (air trench) index contrast regions, a dramatic reduction in the bending radius of otherwise low index contrast waveguides is possible without causing large junction losses through mode mismatch and Fresnel reflection. This air trench technique can be applied to various kind of index contrast system ranging from Δ=0.7% (current PLC technology) to Δ=20% (high refractive index SiON) depending on future demands just by placing air trench at bend. Experimental results show that this is a realistic technique to achieve compact waveguide system using current well-established CMOS technology. The results match vtheoretical simulations.

Total bend length (radius and taper) was reduced by a factor of 5-50 in our silica examples depending on index contrast. Because bending radius is one of the primary factors limiting the density of integration in silica, use of air trench bends such as the ones presented may allow dense integration leading to reduced cost and better yield, while preserving the good fiber coupling and propagation loss properties of silica PLCs.

We also showed an air trench T-splitter as a simple and compact splitter. In this case, precise alignment is required though it is achievable using currently available exposure system.

This air trench waveguide guide has other applications such as BioMEMS (e.g. Evanescent-filed sensor) or Er-doped waveguide amplifier (EDWA).

ACKNOWLEDGEMENTS

Use of the NPACI Cray T-90 supercomputer at SDSC for FDTD simulations is gratefully acknowledged. Shoji Akiyama also wishes to thank Christina Manolatou for use of her well-written FDTD simulation code and MIT Micro Technology Laboratory (MTL) for providing us with lots of useful fabrication techniques and useful discussions.

REFERENCES

[1] T. Miya, "Silica-based planar lightwave circuits: passive and thermally active devices," *IEEE J. of Sel. Topics in Quan. Electron.*, vol. 6, pp. 38-45, Jan. 2000.

[2] E. A. J. Marcatili, "Bends in optical dielectric waveguides," *Bell Sys. Tech. J.*, vol. 48, pp. 2103-2132, Sep. 1969.

[3] M. Heiblum and J. H. Harris, "Analysis of curved optical waveguides by conformal transformation," *IEEE J. of Quan. Electron.*, QE-11, pp. 75-83, Feb. 1975.

[4] D. Rowland, "Nonperturbative calculation of bend loss for a pulse in a bent planar waveguide," *IEE Proc.-Optoelectron.*, vol. 144, pp. 91-96, Apr. 1997.

[5] I.C. Goyal, R.L. Gallawa and A.K. Ghatak, "Bent planar waveguides and whispering gallery modes: a new method of analysis," *J. Lightwave Technol.*, vol. 8, pp. 768-774, May 1990.

[6] M.K. Smit, E.C.M. Pennings, and H. Blok, "A normalized approach to the design of low-loss optical waveguide bends," *J. Lightwave Technol.*, vol. 11, pp. 1737-1742, Nov. 1993.

[7] K. K. Lee, D. R. Lim, L. C. Kimerling, J, Shin, and F. Cerrina, "Fabrication of ultralow-loss Si/SiO_2 waveguides by roughness reduction," *Opt. Lett.*, vol. 26, pp1888-1890, 2001.

[8] K. K. Lee, D. R. Lim, H-C. Luan, A. Anu, J. Foresi, and L. C. Kimerling, "Effect of size and roughness on light transmission in a Si/SiO_2 waveguide: Experiments and model, " *Appl. Phys. Lett.*, vol. 77, pp. 1617-1619, 2000.

[9] M. Loncar, T. Doll, J. Vuckovic, A. Scherer, "Design and fabrication of silicon photonic crystal optical waveguides," *J. Lightwave Technol.*, vol. 18, pp. 1402-1411, 2000.

[10] A. Chuntinan and S. Noda, "Waveguides and waveguide bends in two-dimensional photonic crystal slabs," *Phys. Rev. B*, vol. 62, pp. 4488-4492, 2000.

[11] A. Talneau, L. L. Gouezigou, N. Bouadma, M. Kafesaki, C. M. Soukoulis, and M. Agio, "Photonic-crystal ultrashort bends with improved transmission and low reflection at 1.55μm," *Appl. Phys. Lett.*, vol. 80, 2002.

[12] R. Germann, H. W. Salemink, R. Beyeler, G. L. Bona, F. Horst, I. Massarek, and B. J. Offrein, "Silicon Oxynitride Layers for Optical waveguide Applications," *J. Electrochem. Soc.*, vol. 147. pp. 2237-2241, 2000

[13] R. M. de Ridder, K. Worhoff, A. Driessen, P. V. Lambeck and H. Albers, "Silicon Oxynitride Planar Waveguiding Structures for Application in Optical Communication," *Selected Topics in Quantum Electronics, IEEE Journal.*, vol. 4, pp. 930-937, 1998.

[14] A. del Prado, I. Martil, M. Fernandez, G. Gonzalez-Diaz, "Full composition range silicon oxynitride films deposited by ECR-PECVD at room temperature," *Thin Solid Films*, vol. 343-344, pp. 437-440, 1999.

[15] C. M. M. Denisse, K. Z. Troost, F. H. P. M. Habraken, W. F. van der Weg, and M. Hendriks, "Annealing of plasma silicon oxynitride films," *J. Appl. Phys.*, vol. 69, pp. 2543-2547, 1986.

[16] D. Peters, K. Fischer, and J. Muller, "Integrated optics Based on Silicon Oxynitride Thin Films Deposited on Silicon Substaret for sensor Applications," *Sensors and Actuators A: Physical,* vol. 26, pp. 425-431, 1991.

[17] K. Worhoff, A. Driessen, P. V. Lambeck, L. T. H. Hilderink, P. W. C. Linders, and Th. J. A. Popma, "Plasma enhanced chemical vapor deposition silicon oxinitride optimized for application in integrated optics," *Sensors and Actuators A: Physical,* vol. 74, pp. 9-12, 1999.

[18] M. Popovic, K. Wada, S. Akiyama, H. A. Haus, and J. Michel, *J. Lightwave Technol.*, "Air Trenches for Sharp Silica Waveguide Bends," vol. 20, pp. 1762-1772, 2002.

[19] A. Sakai, G. Hara, and T. Baba, "Propagation Characteristics of Ultrahigh-Δ Optical Waveguide on Silicon-on-Insulator substrate," Jpn. J. Appl. Phys. Vol. 40, pp. L383-L385, 2001.